Hierarchical Hydrodynamic Model Comparisons by a Two Dimensional MOSFET Simulator

C.-F. Yeap*, T. J. Bordelon*, X.-L. Wang*, V. M. Agostinelli*, C. M. Maziar*, A. F. Tasch*, and R. Harkness+
* Microelectronics Research Center, University of Texas at Austin, Austin, TX
+ University of Texas System Center for High Performance Computing, Austin, TX

ABSTRACT

A two-dimensional hierarchical hydrodynamic (HD) model based MOSFET simulator has been developed. The HD equations are solved in the time-dependent (TD) decoupled manner. The simulator has been used to compare the results from nonparabolic, parabolic HD, energy balance, simplified HD, and drift-diffusion (DD) models.

INTRODUCTION

Limitations in simulating hot carrier effects in submicron MOSFET structures using stationary transport models such as the drift-diffusion model and its variants present the motivation for our efforts in developing a simulator based on more complete transport models. A two-dimensional MOSFET simulator based on a hierarchy of transport models ranging from the traditional DD model through various simplified HD to full HD models has been developed on the CRAY YMP at The University of Texas System Center for High Performance Computing. The simulator uses the MINIMOS 4.0 input processor and the DD solution as initial guess to the time-dependent hydrodynamic calculations. The simulator offers a single platform for comparing and contrasting different transport models so that insightful decisions may be made on the trade off between computational efficiency and physical accuracy for device design.

MATHEMATICAL AND NUMERICAL METHODOLOGY

The hierarchical HD equations are scaled by DeMari-type constants and reformulated in terms of (Ψ, η, u, v, w) variables. Different models are realized by adjusting parameters such as α and Ω, and by solving completely or neglecting some terms in the equations.

$$-\nabla\bullet(\nabla\Psi) = p - n + N_d - N_a \tag{1}$$

$$\frac{\partial\eta}{\partial t} + \vec{V}\bullet(\nabla\eta) - \nabla\bullet(\beta_2\mu T\nabla\eta) = -\nabla\bullet(\mu\nabla\Psi_{eff}) - \nabla\bullet\vec{V}^* \tag{2}$$

$$\tau_p\frac{\partial(\beta_1 u)}{\partial t} + \tau_p(\vec{V}\bullet\nabla u) + u = \mu(\nabla_x\Psi_{eff}) - \beta_2 D(\nabla_x\eta) \tag{3}$$

$$\tau_p\frac{\partial(\beta_1 v)}{\partial t} + \tau_p(\vec{V}\bullet\nabla v) + v = \mu(\nabla_y\Psi_{eff}) - \beta_2 D(\nabla_y\eta) \tag{4}$$

$$\frac{\partial w}{\partial t} + \Omega(\vec{V}\bullet\nabla w) + (\Omega\text{-}1)(\vec{V}\bullet\nabla\eta)w + (\Omega\text{-}1)(\nabla\bullet\vec{V})w + \frac{w}{\tau_w} = \vec{V}\bullet\nabla\Psi + \frac{w_o}{\tau_w} + (\Omega\text{-}1)\nabla\bullet(\vec{V}e) + (\Omega\text{-}1)(e\vec{V}\bullet\nabla\eta) \tag{5}$$

where

$$\eta = \ln(n)\ ;\ \vec{V} = u\,\hat{x} + v\,\hat{y}\ ;\ e = 0.5(u^2+v^2)\ ;\ T = (\gamma-1)(w-e)\ ;\ D = \mu T\ ;$$

$$\beta_1 = (1+2\Omega\alpha w)\ ;\ \beta_2 = \frac{(1+\alpha w)}{(1+2\alpha w)}\ ;\ \Psi_{eff} = \Psi - \beta_2(\gamma\text{-}1)w + \beta_2(\gamma\text{-}1)e$$

$$\vec{V}^* = -\tau_p\frac{\partial(\beta_1\vec{V})}{\partial t} - \tau_p(\vec{V}\nabla\bullet)\vec{V}$$

Due to its attractiveness in memory requirement, and its modularity as well as flexibility in coding, the TD decoupled approach is used. A Newton method is utilized to linearize each equation. Stability and convergence of the nonlinear Poisson solution is enhanced by the modified Gummel scheme [1]. The space charge control scheme [2] is employed to handle the coupling between the Poisson and the particle-balance equations, and to relax the severe dielectric time-step restriction. Each equation of the system (Poisson, momentum-balance, energy-balance and particle-balance equations) is iteratively solved within each time-step until self-consistency is achieved. Figure 1 captures the main features of the TD decoupled algorithm.

An implicit one-step time-marching scheme is used to treat the transient nature of the equations. The first-order spatial derivatives are discretized by the second upwind scheme, which has been shown to have an accuracy comparable to higher order methods [3], while center differencing is used for second-order derivatives. The choice of using the relatively slowly varying *ln(n)* rather than *n* as a solution variable has drastically reduced the number of grid points required and, thus, both CPU time and storage requirements [4].

HIERARCHICAL MODEL COMPARISONS

Recently several non-parabolic (NP) HD models have been proposed to achieve better physical accuracy. In contrast to other recently developed models [5,6], Bordelon et al. [7] devised an efficient and simple NP-HD model which requires no additional relaxation times, and predicts a reduction in diffusion and convective energy flux.

Five different model results, namely, nonparabolic HD (NP-HD) , parabolic HD (P-HD), simplified HD which neglects the terms arising from the drift kinetic energy in the momentum-balance equations (S-HD1), simplified HD which neglects thermal diffusion in the momentum-balance equation (S-HD2) and the DD models, are generated for a 0.65 μm L_{eff} simple MOSFET (V_T=0.35V, V_g=1V, V_d=3V) and a 0.48 μm L_{eff} LDD MOSFET (V_T=0.7V, V_g=1V, V_d=2V).

NP-HD: $\gamma = \frac{5}{3}$; $\Omega = 1.3$; $\alpha = 0.5$; e = 0.0 ; neglect $(\vec{V}\bullet\nabla u)$ and $(\vec{V}\bullet\nabla v)$

P-HD: $\gamma = \Omega = \frac{5}{3}$; $\alpha = 0.0$

S-HD1: P-HD, e = 0.0, and neglect $(\vec{V}\bullet\nabla u)$ and $(\vec{V}\bullet\nabla v)$ terms

S-HD2: S-HD1, and $w = w_o$ in particle- and momentum-balance eqns.

D-D: S-HD2, $\tau_p = \mu(\nabla\Psi)$, and $w = w_o$ (not solving energy-balance equation)

Figures 2 and 3 show respectively the strong reaction of the electron energy and lateral velocity before relaxing self-consistently to steady state. In the TD decoupled process, continuation of the energy-dependent momentum relaxation time and the use of the hierarchical models combine to improve our ability to achieve convergence for deep submicron MOSFETs. The S-HD1, also known as the energy balance model, is a good approximation yielding extremely close agreement with the P-HD. Computationally, this translates into a savings of about 40% since there is no need to invert the linear systems generated by the momentum-balance equations.

As shown in Figures 4 and 5, the NP-HD with reduced convective energy flux predicts a higher energy peak than the P-HD. These differences will affect energy based impact ionization calculations even though they have a negligible impact on drain current.

Figures 6 and 7 show the spreading of electrons due to thermal diffusion into the channel. NP-HD yields less spreading due to the reduced thermal diffusion. S-HD2 (similar to solving an energy-balance equation with DD current continuity equations) shows no current spreading even though it gives reasonable estimation of energy profile which may be used to compute a global indicator such as substrate current to monitor energetic carriers. The inadequacy of this approach lies in its inability to predict precisely the location for impact ionization.

SUMMARY

A two-dimensional hierarchical model based MOSFET simulator using the TD decoupled algorithm has been developed. The simulator has been used to confirm the effect of reduced thermal diffusion in the NP-HD model, and examine simplifications which may aid numerical efficiency. Both the NP-HD and S-HD1

(energy balance model) are able to predict relevant physics in a computationally efficient manner. As feature sizes of MOSFETs are aggressively scaled into the deep submicron dimension, the approach of solving an energy-balance equation with DD current continuity equations will not be able to accurately simulate relevant hot carrier phenomena.

REFERENCES

[1] B. S. Polsky and J. S. Rimshans, Solid State Electronics, Vol. 24, pp. 1081-1085, 1981.
[2] J. P. Kreskovsky and H. L. Grubin, J. Comp. Phys., Vol. 68, pp. 420-461, 1987.
[3] E. Fatemi et al., in Computational Electronics, ed. K. Hess et al., pp. 27-32, 1991.
[4] D. Sodini et al., Solid State Electronics, Vol. 29, pp. 969-976, 1986.
[5] D. Chen et al., EDL, Vol. 13, pp. 26-28, 1992.
[6] R. Thoma et al., IEEE T-ED, Vol. 38, pp. 1343-1353, 1991.
[7] T. J. Bordelon et al., Solid State Electronics, Vol. 35, pp. 131-139, 1992.

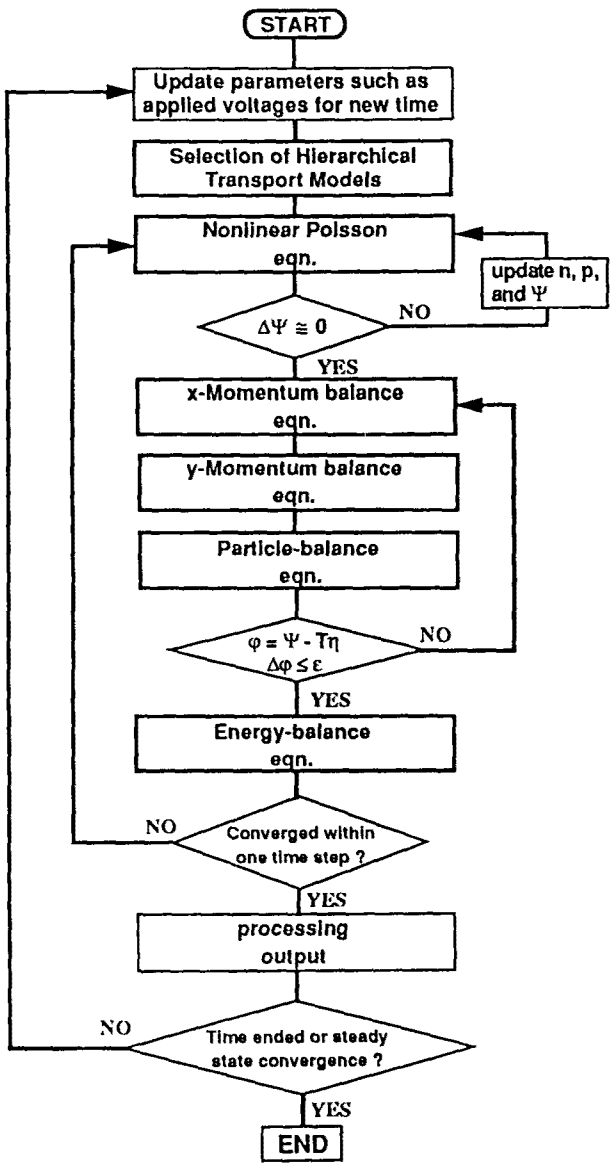

Fig. 1: General flowchart for solving the time dependent hierarchical hydrodynamic equations

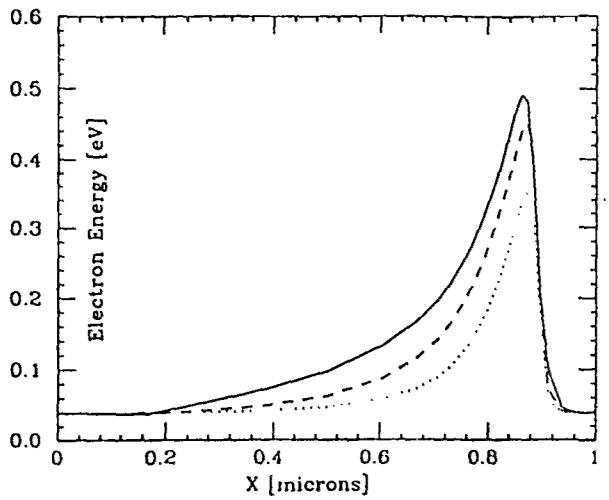

Fig. 2: Temporal evolution of electron energy (dot: t=0.1 ps; dash: t=0.2 ps; solid: steady state)

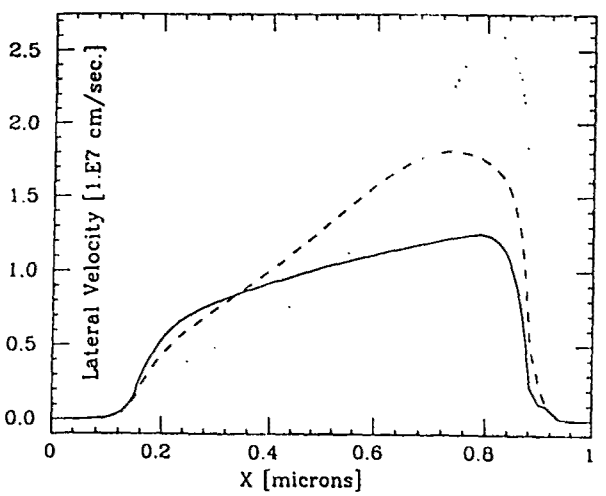

Fig. 3: Temporal evolution of electron velocity (dot: t=0.1 ps; dash: t=0.2 ps; solid: steady state)

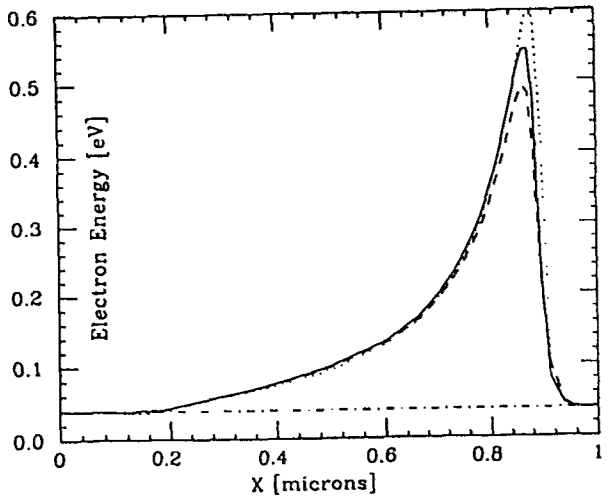

Fig. 4: Hierarchical model comparison of electron energy for the 0.65 L_{eff} MOSFET (solid: NP-HD; dash: P-HD; dot: SHD2; dot-dash: DD)

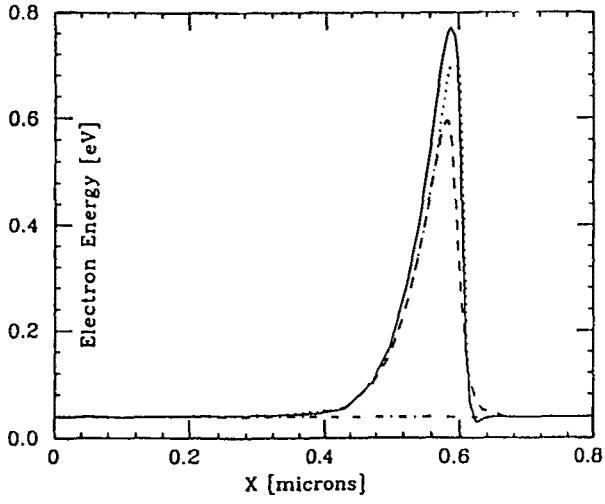

Fig. 5: Hierarchical model comparison of electron energy for the 0.48 L_{eff} LDD MOSFET (solid: NP-HD; dash: P-HD; dot: SHD2; dot-dash: DD)

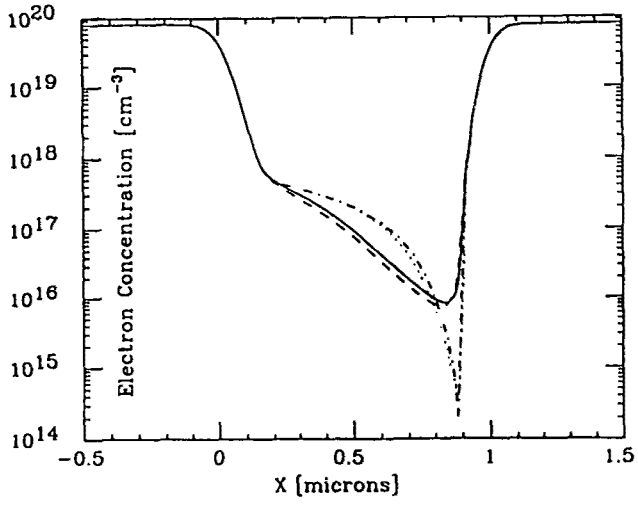

Fig. 6: Hierarchical model comparison of electron concentration for the 0.65 L_{eff} MOSFET (solid: NP-HD; dash: P-HD; dot: SHD2; dot-dash: DD)

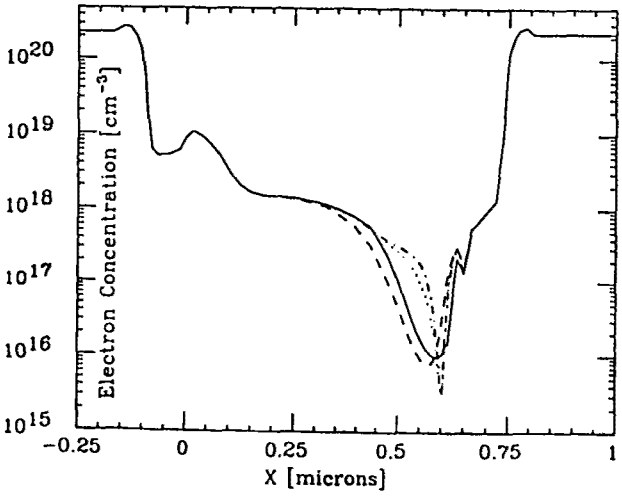

Fig. 7: Hierarchical model comparison of electron concentration for the 0.48 L_{eff} LDD MOSFET (solid: NP-HD; dash: P-HD; dot: SHD2; dot-dash: DD)